



1 Compound winter low wind and cold events impacting the French  
2 electricity system: observed evolution and role of large-scale  
3 circulation

4

5 François Collet<sup>1</sup>, Margot Bador<sup>1</sup>, Julien Boé<sup>1</sup>, Laurent Dubus<sup>2</sup>, Bénédicte Jourdié<sup>2</sup>

6

7 <sup>1</sup>CECI Université de Toulouse, CERFACS/CNRS, Toulouse, France

8 <sup>2</sup>RTE, Paris, France

9

10 Correspondance to : François Collet ([collet@cerfacs.fr](mailto:collet@cerfacs.fr))

11

12

13 **Abstract.** To reach climate mitigation goals, the share of wind power in the electricity production is  
14 going to increase substantially in France. In winter, low wind days are challenging for the electricity system  
15 if compounded with cold days that are associated with peak electricity demand. The scope of this study is to  
16 characterize the evolution of compound low wind and cold events in winter over the 1950-2022 period in  
17 France. Compound events are identified at the daily scale using a bottom-up approach based on two indices  
18 that are relevant to the French energy sector, derived from temperature and wind observations. The frequency  
19 of compound events shows high interannual variability, with some winters having no event and others having  
20 up to 13, and a decrease over the 1950-2022 period. Based on a k-means unsupervised classification technique,  
21 four weather types are identified, highlighting the diversity of synoptic situations leading to the occurrence of  
22 compound events. The weather type associated with the highest frequency of compound events presents  
23 pronounced positive sea-level pressure anomalies over Iceland and negative anomalies west of Portugal,  
24 limiting the entrance of the westerlies and inducing a north-easterly flow bringing cold air over France and  
25 Europe generally. We further show that the atmospheric circulation and its internal variability are likely to  
26 play a role in the observed reduction in cold days, suggesting that this negative trend may not be entirely be  
27 driven by anthropogenic forcings. Despite this suggested role for cold days, the observed decrease in  
28 compound events does not seem to be strongly influenced by the regional atmospheric circulation.

29 **1 Introduction**

30 The transition of the energy system, including the reinforced integration of renewable energy, is  
31 necessary to reduce greenhouse gas emissions in accordance with the Paris Agreement. A recent report from  
32 the French electricity transmission system operator (Réseau de Transport d'électricité, 2023 ; RTE in the



33 following) shows that the national energy transition will rely on a widespread electrification of residential  
34 heating, transport, and the industry, along with improving energy efficiency (e.g., thermal renovation of  
35 buildings). Therefore, the electricity demand is projected to increase from 475TWh in 2019 to 580-640 TWh  
36 in 2035, according to scenarios in which France meets its energy transition goals (see scenarios A in RTE,  
37 2023). In light of the future electricity demand, France has expressed its intention to significantly expand its  
38 wind energy capacity in the coming decades. Onshore wind power capacity is projected to increase from  
39 20GW in 2022 to 30-39GW and substantial additional offshore wind farms are also planned, with a total  
40 projected capacity of 18GW by 2035 compared to 0.5GW in 2022 (RTE, 2023).

41 The production and demand of electricity can be affected by a range of climate conditions over multiple  
42 time scales. In terms of electricity demand during winter, France is known to be one of the most temperature  
43 sensitive among European countries (Bloomfield et al., 2020a). This is mainly explained by the high usage of  
44 electricity for residential heating, which is expected to increase over the next decades (RTE, 2023). Hence,  
45 cold events will likely continue being associated with peak electricity demand based on the projections of the  
46 French future electricity system (RTE, 2023). Besides, part of the electricity production in France relies on  
47 renewable energies that are sensitive to climate conditions including wind speed, solar radiations, and river  
48 flows. As the proportion of renewable energy in the French electricity mix is set to rise, the electricity  
49 production will be more importantly affected by climate variability. In particular, it is anticipated that a higher  
50 proportion of wind power in the electricity mix may lead to higher risks for the production of electricity,  
51 especially during low wind events. This is particularly the case in winter, when solar generation represent a  
52 smaller share of the electricity production (Grams et al., 2017; Otero et al., 2022b). Hence, in France, it can  
53 be challenging to ensure adequate electricity supply and demand due to the occurrence of multivariate  
54 compound events (Zscheischler et al., 2020), such as low wind and cold events, which can create stressful  
55 situations. The aim of this study is to characterize compound low wind and cold events in France.

56 Overall, there is little information in the literature on the observed evolution of compound low wind  
57 and cold events in France and Europe. A body of studies focuses on related events using electricity supply and  
58 production data. For instance, an electricity supply drought is defined by a sequence of days with low  
59 renewable electricity production and high electricity demand (Raynaud et al., 2018). Most of these studies  
60 focus on the characterization of the statistical properties of these events (Otero et al., 2022a, b; Raynaud et al.,  
61 2018; Tedesco et al., 2023) or their drivers (Bloomfield et al., 2020a; Ravestein et al., 2018; Thornton et al.,  
62 2017; van der Wiel et al., 2019a, b). Only a limited number of these studies focus on their temporal evolution  
63 in the context of climate change. Van der Wiel et al. (2019a) show that the frequency of electricity supply  
64 droughts in Europe is reduced in a 2°C warmer world compared to present day conditions, using projections  
65 from two global climate models. Although there is a gap in the understanding of the past evolution of  
66 compound low wind and cold events, changes in low wind or cold events have been investigated  
67 independently. Rapella et al. (2023) showed that the number of low wind events decreases in the ERA5  
68 reanalysis over the 1950-2022 period. However, they focus only on offshore regions such as the Bay of Biscay,



69 the North Sea, and the Channel, in summer and at the annual scale. Focusing on cold temperature conditions  
70 in winter, there is evidence that the frequency and intensity of cold spells have decreased over the last decades  
71 in Europe (Cattiaux et al., 2010; Seneviratne et al., 2021; Van Oldenborgh et al., 2019). While there is clear  
72 evidence that climate change leads to a reduction in cold events, there are still major uncertainties regarding  
73 low wind events. It is therefore difficult to anticipate how compound low wind and cold events may change  
74 in the coming decades as there is a lack of understanding of their past evolution. An objective of this study is  
75 to assess the evolution of these compound events in the observational record.

76 This work also focuses on the influence of the regional atmospheric circulation on the occurrence and  
77 evolution of compound low wind and cold events. The atmospheric circulation is an important driver of  
78 temperature variability (Plaut and Simonnet, 2001) and wind speed variability (Najac et al., 2009) in France,  
79 and here we aim to further assess its influence on compound events in winter. In the literature, different  
80 approaches have been used to explore the influence of the atmospheric circulation and its variability in  
81 favoring particular meteorological situations that affect the electricity sector. This includes identifying weather  
82 regimes of interest (Otero et al., 2022b; van der Wiel et al., 2019b; Tedesco et al., 2023), targeted circulation  
83 types (Bloomfield et al., 2020b), and circulation regimes based on large-scale conditions leading to critical  
84 situations for the electricity system such as days with extremely high electricity demand (Thornton et al.,  
85 2017). Tedesco et al. (2023) showed that compound low wind and cold events in France are mostly associated  
86 with positive anomalies of geopotential height at 500hPa over Iceland and negative anomalies over the Azores.  
87 Otero et al. (2022b) showed that situations of limited production of electricity from wind and solar energies  
88 co-occurring with cold events are mostly associated with positive anomalies of geopotential height at 500hPa  
89 over the North Sea region.

90 Finally, we investigate to what extent the regional atmospheric circulation and its variability contribute  
91 to the past evolution of compound low wind and cold events in France. Several studies found that recent  
92 changes in the large-scale circulation play a role in the winter trend in mean temperature across Europe (Deser  
93 and Phillips, 2023; Sippel et al., 2020; Saffioti et al., 2016), and in the decreasing occurrence and intensity of  
94 cold extremes (Horton et al., 2015; Terray, 2021). Using a dynamical adjustment approach based on  
95 observation data (Terray, 2021), we explore the role of the changes in atmospheric circulation in the observed  
96 trend in compound low wind and cold events in France.

97 This paper is organized as follows: section 2 presents the data and the method used, section 3 presents  
98 the main results and section 4 includes a conclusion and discussion of the findings.

## 99 **2 Data and Method**

100 First, the data and the methodology used to identify low wind events, cold events, and compound low  
101 wind and cold events responsible for stressful situations for the adequacy between electricity demand and  
102 supply in France are described.



## 103 2.1 Observations and reanalyses of atmospheric variables

104 The ERA5 reanalysis data (Hersbach et al., 2020) is used over the period 1950-2022. ERA5 is available  
105 on a regular grid with a resolution of about 30 km in Europe. In particular, the hourly wind speed (at 100 m)  
106 and the daily near-surface air temperature (at 2m) are used for the calculation of the wind capacity factor and  
107 temperature indices, respectively (section 2.3 and 2.4). Daily mean sea level pressure is also used for  
108 classification of the large-scale circulation into weather types (see section 2.6) and dynamical adjustment  
109 (section 2.7). In addition to the ERA5 reanalysis, wind and temperature data from the MERRA-2 reanalysis  
110 (Gelaro et al., 2017) are considered. MERRA-2 is available at a horizontal resolution of about 60 km over  
111 Europe, over the 1980-2022 period. Hourly near-surface air temperature and wind (at 50 m) are used. We also  
112 consider in situ temperature observations from the gridded E-OBS dataset (Cornes et al., 2018) over the 1950-  
113 2022 period, available on a regular grid with a horizontal resolution of about 30 km in Europe.

114 This study is mainly focused on an extended winter period, from November to March, when compound  
115 low wind and cold events occur in France. By convention, hereafter, winter 1951 corresponds to the period  
116 from November 1950 to February 1951 and so one.

## 117 2.2 Observations of the wind power production and electricity demand in France

118 Hourly observed data for the wind power production and electricity demand in France are taken from the  
119 `écO2mix` dataset ([https://odre.opendatasoft.com/explore/dataset/eco2mix-national-cons-  
120 def/information/?disjunctive.nature](https://odre.opendatasoft.com/explore/dataset/eco2mix-national-cons-def/information/?disjunctive.nature)), over the 2012-2020 period. The French wind power installed capacity is  
121 available at 3-monthly time intervals over the 2012-2020 period at [https://www.statistiques.developpement-  
122 durable.gouv.fr/publicationweb/549](https://www.statistiques.developpement-durable.gouv.fr/publicationweb/549). Hourly observed wind capacity factor is calculated using the hourly  
123 observed wind power production from `écO2mix`, which is divided by the wind power installed capacity in  
124 France of the corresponding 3-monthly interval.

## 125 2.3 Wind capacity factor index

126 Several studies (Bloomfield et al., 2022; Jourdir, 2020; Olauson, 2018; Staffell and Pfenninger, 2016)  
127 demonstrated that it is possible to calculate hourly wind capacity factor at country-scale with a good accuracy  
128 using wind speed from reanalysis data in Europe. Here, we use a similar approach to calculate the French wind  
129 capacity factor index over the 1951-2022 period.

130 This approach requires information at each wind farm site, which are taken from The Wind Power  
131 database (<https://www.thewindpower.net/>), including the location, rated power, hub height, and power curves  
132 at each site (upon availability). Only wind farms operational in 2021 are used (i.e., those with “in production”  
133 status). This represents a total number of 1661 wind farms and a total installed capacity of 19GW. Wind farms  
134 and related wind power installed capacity are concentrated in the North-East of France (Figure 1a). While the  
135 installed wind power capacity is fairly accounted for in this database, there is a substantial amount of missing



136 data regarding the hub heights and the power curves (~29% and ~7% of wind farms, respectively). Missing  
137 data is filled in following the methodology introduced in Jourdi er (2020), which broadly consists in taking  
138 characteristics from wind farms identified as similar in terms of rated power, rated diameter, rated wind speed,  
139 cut-in and cut-off wind speed.

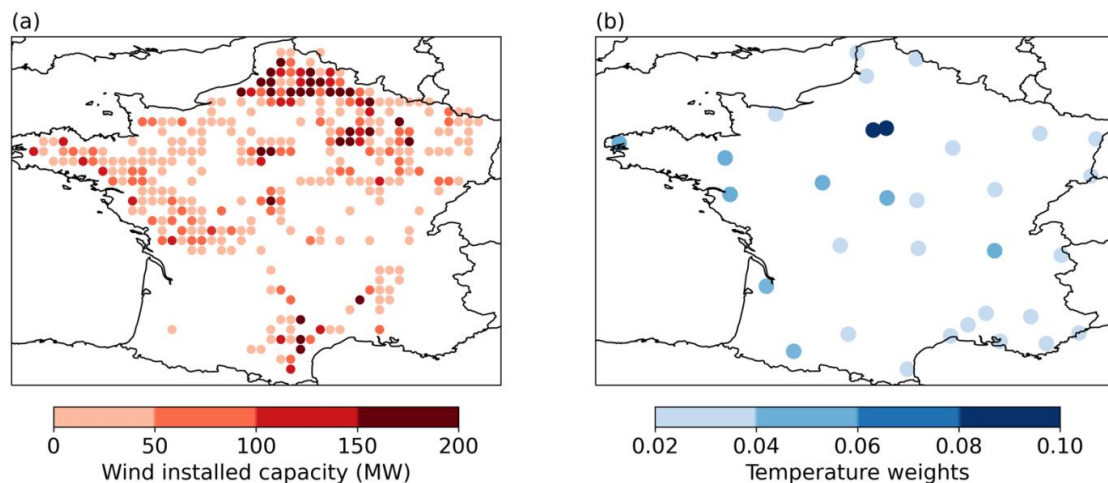
140 Calculation of the wind capacity factor first requires interpolating ERA5 hourly wind speed from 100  
141 m at each wind farm's hub height. This is done using a power law ( $\alpha=0.14$ ; Manwell, 2010; van der Wiel et  
142 al., 2019a). Then, using the power curve of each wind farm, wind speed at the hub height is converted into  
143 power production. Finally, the hourly wind capacity factor over France is estimated by summing the power  
144 production from all wind farms, and dividing this total power production by the total installed capacity.  
145 Finally, hourly wind capacity factors are averaged to daily values to further identify low wind days (section  
146 2.5).

147 The daily wind capacity factor index computed with this approach is extremely well correlated with  
148 observations over their 9 common winters ( $r=0.99$ , Figure 2a), highlighting the relevance of using ERA5 data  
149 in this context.

#### 150 **2.4 Temperature index representative of the demand in electricity**

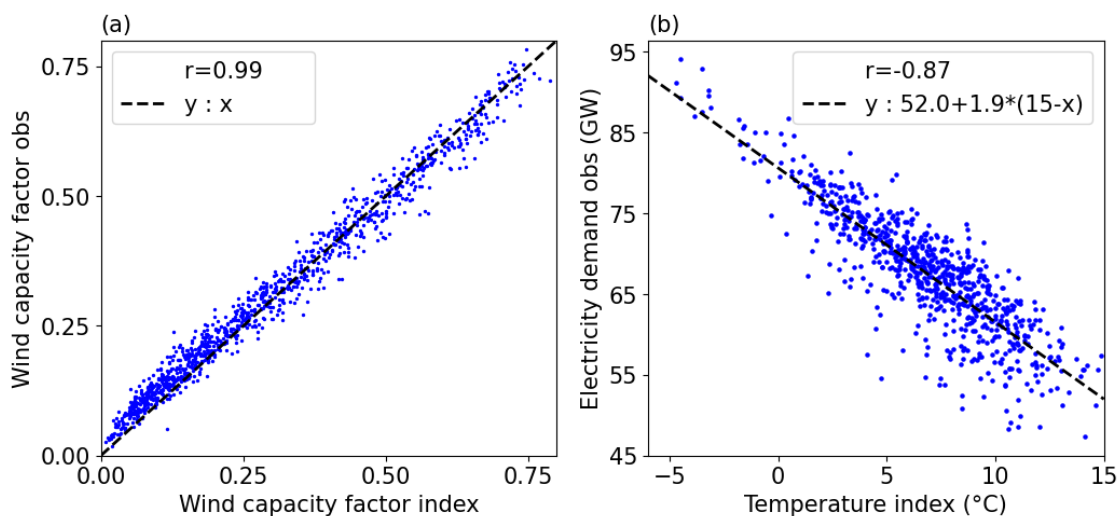
151 The temperature index is defined following an approach used operationally by RTE that consists in  
152 calculating a weighted average of temperature data from 32 cities in France (Figure 1.b), which is  
153 representative of the electricity demand in France. First, the near-surface air temperature in ERA5 at the grid-  
154 cell closest to each city location is selected. Then, temperatures are corrected based on the difference between  
155 the elevation of the grid cell and the elevation of the in situ station for each city, assuming a vertical gradient  
156 of temperature of  $-6.5^\circ\text{C}/\text{km}$ . Finally, the weighted average of temperature at the 32 locations is calculated  
157 over the 1950-2022 period.

158 A strong anti-correlation of  $-0.82$  is found between the temperature index and the observed electricity  
159 demand in winter (Figure 2b). This highlights the relevance of the temperature index as a proxy for the French  
160 demand in electricity.



161

162 Figure 1: (a) Spatial distribution of the wind power installed capacity (MW) in France in 2021 from the  
 163 WindPower.net dataset used for the calculation of the wind capacity factor index. (b) Location of the 32 French  
 164 cities and associated weights (no unit) used for the calculation of the temperature index.



165

166 Figure 2: (a) National French wind capacity factor index as calculated with ERA5 (no unit; X-axis) versus  
 167 observations (no unit; Y-axis) in winter over the 2012-2020 period. The correlation coefficient is given in the  
 168 top left corner, and the black dotted line represents the  $y:x$  function. (b) Temperature index as calculated in  
 169 ERA5 ( $^{\circ}\text{C}$ ; X-axis) versus observations of the electricity demand (GW; Y-axis) in winter over the 2012-2020  
 170 period, excluding week-ends and bank holidays. The correlation coefficient is given in the top right corner.  
 171 The linear regression line between the temperature index and the electricity demand observations is shown by  
 172 the black dashed line. The corresponding linear regression equation, in the form  $y=y(15^{\circ}\text{C})+a*(15^{\circ}\text{C}-x)$ ,  
 173 where  $15^{\circ}\text{C}$  is the threshold of residential heating and  $a$  the thermosensitivity of the electricity demand, is  
 174 shown in the top right corner.

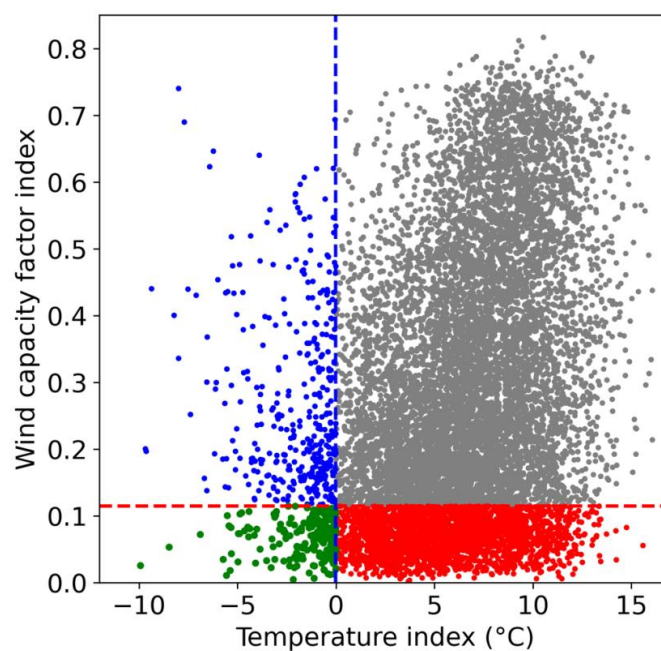




## 175 2.5 Identification of low-wind days, cold days and associated compound events

176 In this study, compound low wind and cold events are defined as days when cold temperature and low  
177 wind conditions co-occur (green points in Figure 3). Cold days are defined here as days with the temperature  
178 index below 0°C, corresponding to the 5th percentile of the distribution of the temperature index in winter  
179 (blue points in Figure 3). Low wind days (red points in Figure 3) are defined as days with a wind capacity  
180 factor index below a certain threshold (here the 23th percentile), which corresponds to a wind capacity factor  
181 of 0.15 in the distribution of observations in winter.

182



183

184 Figure 3: Wind capacity factor index (no units; Y-axis) and temperature index (°C; X-axis) calculated with  
185 ERA5 for each winter day over the 1951-2022 period. Red and blue dashed lines show the thresholds used to  
186 identify low wind days and cold days (red and blue points, respectively). Compound low wind and cold events  
187 are identified by the green dots.

## 188 2.6 Classification into weather types

189 A classification of mean sea-level pressure fields on low wind days is conducted using the k-means  
190 unsupervised classification method (e.g., Cassou, 2008; Falkena et al., 2020). This allows classifying daily  
191 synoptic conditions into different large-scale atmospheric circulation types, or weather types. Here, low wind  
192 days solely are considered for the classification instead of compound low wind and cold events because the  
193 corresponding sample size is larger (2549 days compared to 182 days, respectively; see Figure 3, Figure 4b,



194 and further discussions in section 3). However, in a second phase, we assess how cold days and therefore  
195 compound events are distributed across the different weather types leading to low wind days.

196 This classification algorithm is first applied repeatedly for different domains and number of clusters.  
197 The objective is to minimize locally the ratio of intra-type to inter-type variance of the temperature index,  
198 while keeping a reasonable number of weather types. Thanks to this procedure, the classification of low wind  
199 days that allows for the best differentiation of the temperature index is chosen. This procedure leads to a  
200 domain whose limits are [30°W-30°E/33°S-70°N], which covers the North-Western Europe region, and a total  
201 number of four clusters.

## 202 **2.7 Dynamical adjustment**

203 The main objective of dynamical adjustment is to derive an estimate of the contribution of atmospheric  
204 circulation to the variations of a variable of interest (Terray, 2021; Deser et al., 2016; Sippel et al., 2019). In  
205 this study, we use dynamical adjustment to estimate the contribution of atmospheric circulation to the  
206 variations of cold days, low wind days, and compound events. Hereafter, the contribution of atmospheric  
207 circulation is referred to as the dynamic component.

208 First, we estimate the dynamic component of the wind capacity factor and temperature indices. To that  
209 purpose, the constructed analogue approach is used (Terray, 2021; Boé et al., 2023; Deser et al., 2016).  
210 Following Lorenz (1969), analogues are defined as days with very similar atmospheric circulation. As finding  
211 genuinely good analogues in a finite database could be difficult, synthetic analogues can be constructed  
212 through the linear combination of the atmospheric circulation corresponding to a large number of more or less  
213 good analogues (Van Den Dool, 1994).

214 First, for each target day of the winters 1951-2022, the 1500 closest analogues are searched in winter  
215 using the Euclidean distance calculated with ERA5 mean sea-level pressure interpolated on a 2°x2° grid on  
216 the North-Western Europe domain (section 2.6). The winter of the target day is excluded from the search pool.  
217 Then for each target day, a subset of 1300 analogues are randomly selected from the 1500 analogues, and the  
218 optimal linear combination of this subset of 1300 analogues that best matches the mean sea level pressure of  
219 the target day is calculated. This allows obtaining a constructed analogue for the target day. This procedure is  
220 repeated 50 times, to obtain 50 constructed analogues for each target day and the corresponding 50 sets of  
221 optimal weights. While the 50 constructed analogues of each target day have very similar atmospheric  
222 circulation to the target day, this procedure, together with the large number of analogues used allows us to  
223 sample different land surface and ocean conditions that might otherwise influence the estimate of the dynamic  
224 components (Terray, 2021).

225 For each target day, the wind capacity factor and the temperature indices are then reconstructed by  
226 applying the same set of optimal linear weights to the corresponding wind capacity factor index and detrended  
227 anomalies of the temperature index, respectively. There are 50 reconstructions of the wind capacity factor and  
228 the temperature index per day over the winters 1951-2022. As we are interested in separating the trend due to



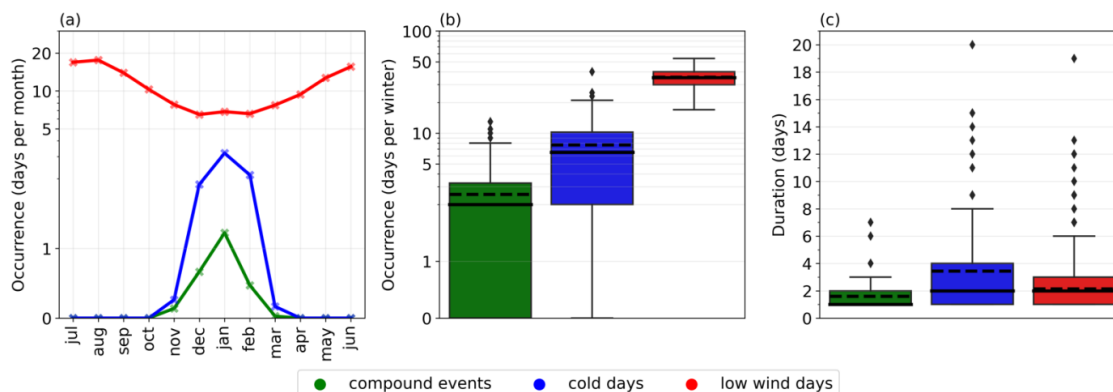


229 large-scale circulation from thermodynamically-forced changes, an estimate of the forced trend of the  
 230 temperature index anomaly for each winter month is removed before applying the dynamical adjustment. This  
 231 low-frequency trend is estimated using a low-frequency LOESS smoother as done in Terray (2021). Finally,  
 232 a best estimate of the dynamic component of the wind capacity factor index and the temperature index are  
 233 derived by averaging the 50 reconstructions of the wind capacity factor index and the temperature index,  
 234 respectively.

235 Finally, the dynamic component of low wind days and cold days is defined using the same thresholds  
 236 as for the definition of cold days and low wind days (i.e., the 5th percentile and the 23th percentile,  
 237 respectively; section 2.5). This allows the dynamic component of compound events to be identified as days  
 238 when both the dynamic component of low wind days and cold days occur.

### 239 3. Results

#### 240 3.1 Climatological characteristics and observed evolution of compound low wind and cold events



241  
 242 Figure 4: (a) Monthly mean number of compound low wind and cold events (green), cold days (blue), and low  
 243 wind days (red); Distributions of (b) the number of days per winter and (c) duration of compound low wind  
 244 and cold events, cold days, and low wind days in winter over the 1951-2022 period in ERA5. The solid line  
 245 and the dashed line in the boxplots in (b) and (c) show the median and the average, respectively.

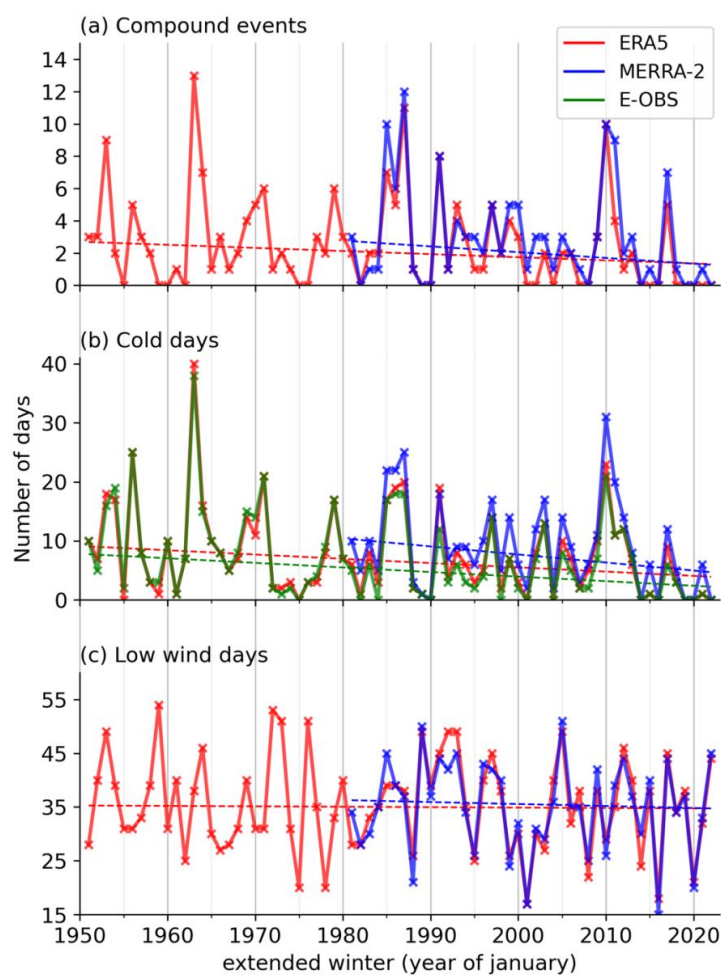
246  
 247 There is a clear seasonality in the occurrence of compound events, which are concentrated in winter  
 248 (November to March; Figure 4a). This is well explained by the seasonality of cold days, which occur from  
 249 November to March in France. Conversely, low wind days are less frequent in winter, with an average of 7  
 250 days for winter months compared to an average of 13 days for other months.

251 The median number of compound events per winter (2 days; Figure 4b) is a third of the median number  
 252 of cold days per winter (6 days; Figure 4b). The median number of low wind days per winter reaches 35 days,  
 253 and is therefore substantially higher than for compound events and cold days. In terms of year-to-year  
 254 variability, we find that the number of compound events ranges from 0 to 13 days per winter, while there are



255 from 0 to 40 cold days and 17 to 54 low wind days. When compared to the mean, the interannual variability  
 256 is thus higher for the occurrence of compound events and cold days compared to low wind days.

257 On average in winter, the duration of compound events is estimated to be around 2 consecutive days, 3  
 258 days for cold days and 2 days for low wind days (Figure 4c). The maximum duration of compound events is  
 259 7 consecutive days, corresponding to the period between 17 and 23 January 1987, at the end of a severe 13-  
 260 day cold spell. Overall, compound low wind and cold events are relatively rare and generally short-lived, but  
 261 they can last for a few days and up to a week occasionally.



262  
 263 Figure 5: Interannual evolution of the number of (a) compound low wind and cold events, (b) cold days, (c)  
 264 and low wind days per winter in ERA5 (in red; 1951-2022), MERRA2 (in blue; 1981-2022) and EOBS (in  
 265 green; 1951-2022) datasets. Dashed lines show the linear trend (calculated with the Theil-Sen estimator; see  
 266 Table 1 for the slope value and associated significance).

267



Data	ERA5		MERRA-2		E-OBS	
Time period	1951-2022	1981-2022	1951-2022	1981-2022	1951-2022	1981-2022
Compound events	-0.19 (0.02)	-0.43 (0.01)	/	-0.36 (0.1)	/	/
Cold days	-0.72 (0.02)	-1.03 (0.08)	/	-1.36 (0.08)	-0.78 (0.0)	-0.67 (0.16)
Low wind days	-0.08 (0.59)	-0.45 (0.48)	/	-0.37 (0.72)	/	/

268

269 Table 1: Trend (slope in days/decade) and associated p-value, in the number of compound low wind and cold  
 270 events, cold days, and low wind days in ERA5, MERRA-2 and E-OBS over their respective time period (as  
 271 indicated in the first row). The slope is calculated with Theil-Sen estimator and the p-value with the Mann-  
 272 Kendall test. Significant trends with  $p < 0.05$  are highlighted with grey shading. Empty cells correspond to  
 273 missing data.

274 Further looking into the year-to-year differences in the number of compound low wind and cold events,  
 275 we find substantial interannual variability (Figure 5a). Some winters stand out as extreme cases, such as 1963,  
 276 1985, 1987, and 2010. In particular, the exceptional winter 1963, is the most extreme winter with 13 days of  
 277 compound events (Figure 5b). Winter 1963 is the coldest winter ever recorded over Western Europe (Hirschi  
 278 and Sinha, 2007) and our results further show that low wind days were co-occurring for some of its cold days.  
 279 Overall, there is a good agreement between ERA5 and MERRA-2 over the shorter 1981-2022 period. This  
 280 includes the characterization of the most extreme winters in terms of compound events, although MERRA2  
 281 generally shows a slightly higher number of compound events per winter.

282 The interannual variability of compound events is primarily driven by the variability of cold days  
 283 compared to the variability of low wind days ( $r=0.86$  and  $r=0.19$  in ERA5, respectively; Figure 5a,b). In  
 284 particular, the highest numbers of compound events are found in years also characterized by the highest  
 285 numbers of cold days, but not necessarily in years with the highest numbers of low wind days (e.g., 1963,  
 286 1987, 2010, Figure 5a,b,c). This might be related to the larger sample of low wind days per winter on average  
 287 compared to the number of cold days, as defined in this study (section 2.5).

288 Over the 1951-2022 period, there is a significant decrease in the number of compound events per winter  
 289 in ERA5 (-0.19 days per decade; Figure 5a and Table 1). Over the shorter period in common between ERA5  
 290 and MERRA2, compound events have also decreased significantly in ERA5, and at a higher rate (-0.43 days  
 291 per decade). MERRA-2 shows a slightly weaker decrease in compound events (-0.36 days per decade)  
 292 compared to ERA5, which is not significant at the 0.05 level ( $p=0.10$ ). In terms of low wind days, no trend is

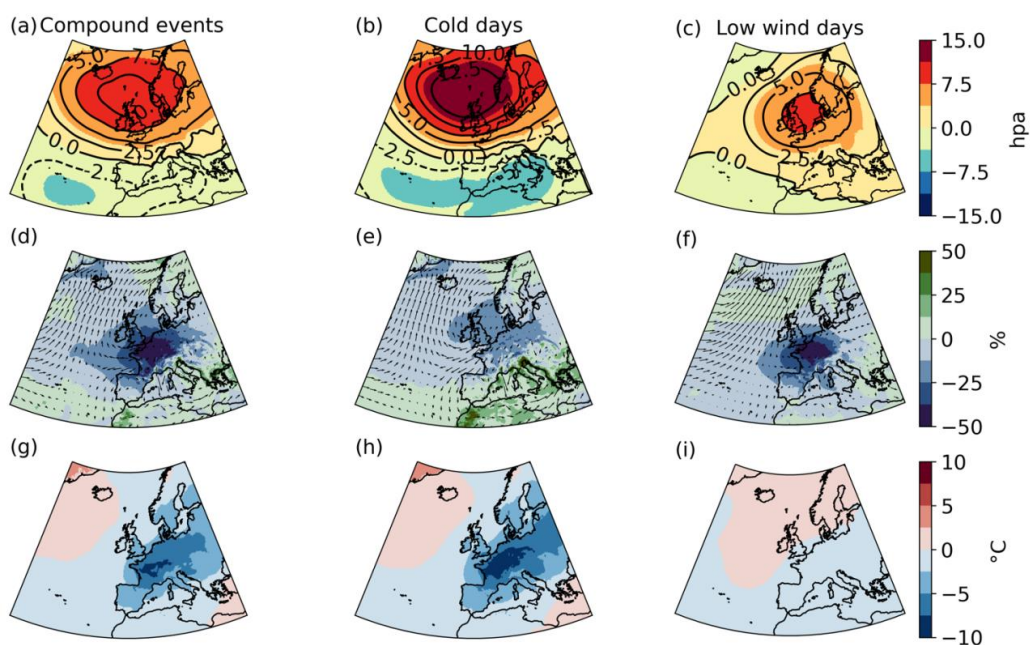


293 detected in ERA5 over both the longer and shorter periods, and both reanalyses agree on the absence of a  
294 trend. Conversely, cold days have significantly decreased over the longer period in both the ERA5 reanalysis  
295 and the E-OBS observations, and at a similar rate of -0.72 and -0.78 days per decade (respectively; Figure 5b  
296 and Table 1). Interestingly, over the shorter period in common with ERA5, MERRA2 and EOBS, the  
297 significance of the negative trend is lost, suggesting that this period might be too short for the influence of  
298 anthropogenic forcings to emerge from internal variability, contrary to what is observed on the longer period.

### 299 **3.2 Role of large-scale circulation.**

300 On average, the synoptic conditions leading to the occurrence of compound low wind and cold events  
301 are characterized by strong positive mean sea-level pressure anomalies over the British Isles and relatively  
302 less intense negative anomalies centred on the Azores (Figure 6a). Overall, the average large-scale circulation  
303 during compound events is very well spatially correlated with that of cold days (Figure 6b), but the intensity  
304 of the positive anomalies and associated pressure dipole are weaker in the case of compound events. The  
305 anomalies in mean sea-level pressure are somehow different during low wind days compared to compound  
306 and cold events. Positive sea level pressure anomalies are found further south over the North Sea, with  
307 relatively lower intensity, and the negative anomalies over the Azores are not as clear (Figure 6c).

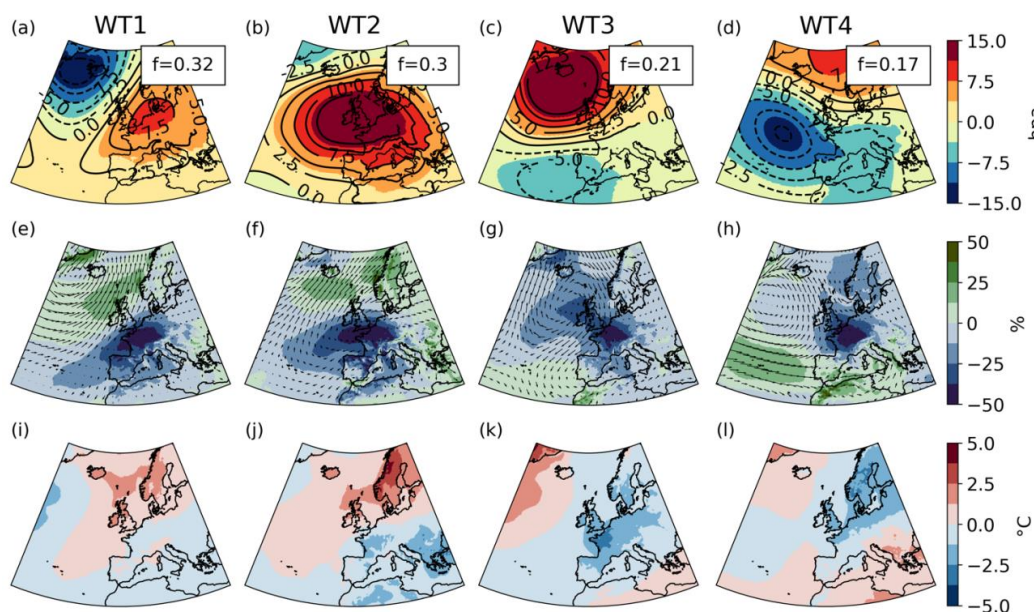
308 By definition, during compound low wind and cold events, France experiences calm and cold  
309 temperature conditions. On average during compound events, the negative anomalies of wind speed and  
310 temperature expand over a wider domain, comprising Germany and the British Isles, with anomalies up to -  
311 40% and -7.5°C, respectively (Figure 6d,g). The negative temperature anomalies over France and surrounding  
312 countries are slightly weaker during compound events compared to cold days (Figure 6g,h). These cold  
313 anomalies are induced by a north-easterly flow advecting cold polar air towards western Europe. During cold  
314 days, and compared to compound events, the negative anomalies in wind speed are less intense, the advection  
315 of cold air is stronger, and thus colder temperatures are experienced over western Europe. During low wind  
316 days, negative wind anomalies are found over western Europe, with intensities rather similar to those during  
317 compound events, along with neutral temperature anomalies (Figure 6f,i). It is important to acknowledge that  
318 these average climate conditions might hide a variety of different regional atmospheric circulations, further  
319 explored in the following using a weather type analysis.



320

321 Figure 6: Composite of (a,b,c) sea-level pressure anomalies (hPa) with solid and dashed contours  
 322 corresponding to positive and negative anomalies respectively, (d,e,f) 100 m wind speed relative anomalies  
 323 (% of climatological mean; shadings) and wind direction (arrow), and (g,h,i) near-surface air temperature  
 324 anomalies, in average during (a,d,g) compound low wind and cold events, (b,e,h) cold days, and (c,f,i) low  
 325 wind days. The anomalies are calculated over the 1951-2022 period in ERA5.

326



327

328





329 Figure 7: Composite of (a,b,c,d) sea-level pressure anomalies (hPa) with solid and dashed contours  
330 corresponding to positive and negative anomalies respectively, (e,f,g,h) 100 m wind speed relative anomalies  
331 magnitude (% of climatological mean; shadings) and wind direction (arrows), and (i,j,k,l) near-surface air  
332 temperature anomalies corresponding to the weather types (a,e,i) WT1, (b,f,j) WT2, (c,g,k) WT3 and (d,h,l)  
333 WT4. The anomalies are calculated over the 1951-2022 period in ERA5. The frequency (f) of the weather  
334 types is shown in the upper right corner in panels a,b,c,d.

335

336 The four weather types obtained with the k-means algorithm (section 2.6) help to identify the most  
337 favorable synoptic situations leading to the occurrence of compound low wind and cold events in France, and  
338 over western Europe more generally.

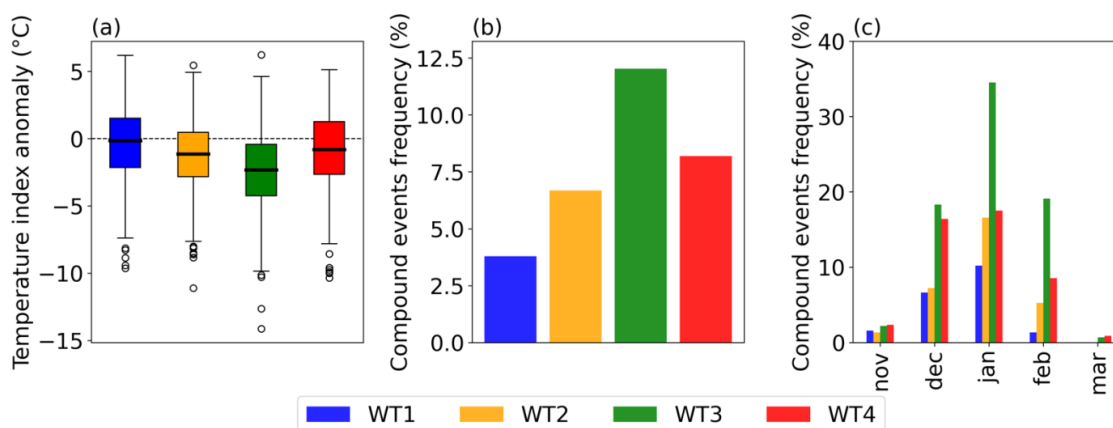
339 The frequency of weather types is rather similar, and ranges from 0.17 (WT4) to 0.32 (WT1). While all  
340 four weather types are characterized by low wind and cold temperatures in France (by definition), they reveal  
341 a diversity of regional atmospheric conditions (Figure 7):

- 342 • WT1 is characterized by positive sea-level pressure anomalies over the Netherlands and northern  
343 Germany, and negative anomalies over Iceland. The positive anomalies block the entry of the  
344 westerlies at the western border of Europe and deviate them further north, thus advecting relatively  
345 warm and humid air over northern Europe, and inducing a substantial decrease in wind speed along  
346 with cold anomalies in France and western Europe.
- 347 • WT2 shares blocking-like characteristics with WT1, but with more intense positive sea level  
348 pressure anomalies and over a wider domain extending further west, pushing the negative SLP  
349 anomalies further to the north-west corner of the domain. As in WT1, the westerlies are derived  
350 north of Europe, inducing a similar dipole of warmer temperatures in the north and colder  
351 temperatures under the positive pressure anomalies. In France and southern Europe in general, and  
352 compared to WT1, the negative anomalies in wind and temperature are enhanced because of the  
353 amplified positive pressure anomalies.
- 354 • WT3 shows pronounced positive sea-level pressure anomalies over Iceland and negative anomalies  
355 west of Portugal. This WT resembles the most to the average atmospheric conditions during  
356 compound events (Figure 6a). The dipole of pressure anomalies results in a strong north to north-  
357 easterly flow advecting cold air masses from Scandinavia to France. This weather type is associated  
358 with the coldest temperatures over France compared to the other weather types, and generally over  
359 the entire European domain that also experiences low wind conditions.
- 360 • WT4 is rather different from WT1, WT2 and WT3 as it is characterized by substantial negative  
361 sea-level pressure anomalies in the eastern Atlantic and positive anomalies over the Norwegian  
362 Sea. These pressure anomalies induce low wind conditions in France and generally the northern  
363 part of Europe, and a reinforcement of the westerlies in the southern part of the domain. This is





364 associated with colder temperatures in the north, including the northern part of France, and positive  
 365 or low temperature anomalies in south-western Europe.  
 366



367  
 368 Figure 8: (a) Distribution of temperature index anomalies for each weather type (WT; as defined in Figure 7  
 369 and indicated in inserted legend); (b) Frequency of compound low wind and cold events for each weather type  
 370 (in % of the weather type size). (c) Frequency of compound low wind and cold events for each weather type  
 371 and each individual winter month (in % of the weather type size for a given month). The anomalies and  
 372 frequencies are calculated over the 1951-2022 period in ERA5.

373  
 374 The temperature index shows a substantial intra-type and inter-type variability (Figure 8a). WT3 is the  
 375 coldest weather type over France overall, with the lowest median of the temperature index. Yet, all weather  
 376 types present very cold days, with anomalies as large as -10°C for WT1 and WT4, and -14°C for WT3. The  
 377 frequency of compound events when a particular weather type occurs varies from 4% in WT1 to 12% in WT3,  
 378 while WT2 and WT4 present similar values of 7% and 8% (Figure 8b). Importantly, the weather type WT3,  
 379 which is associated with the highest frequency of compound events, also leads to negative anomalies in wind  
 380 speed and temperature across Europe (Figure 7c,g,k). It suggests that this weather type might challenge the  
 381 electricity system on a larger scale than just in France.

382 The frequency of compound events in each weather types shows important monthly variations. For all  
 383 weather types, the frequency of compound events is higher in January, when climatological temperature  
 384 reaches the lowest values, compared to other months (Figure 8c). This is especially the case for WT3, for  
 385 which nearly 35% of days occurring in January are compound events. This important role of the temperature  
 386 seasonality within each weather type is consistent with the overall seasonality of compound events discussed  
 387 in section 3.1.

388  
 389



WT1	WT2	WT3	WT4
0.0 (0.78)	0.56 (0.16)	-0.27 (0.29)	-0.59 (0.01)

390

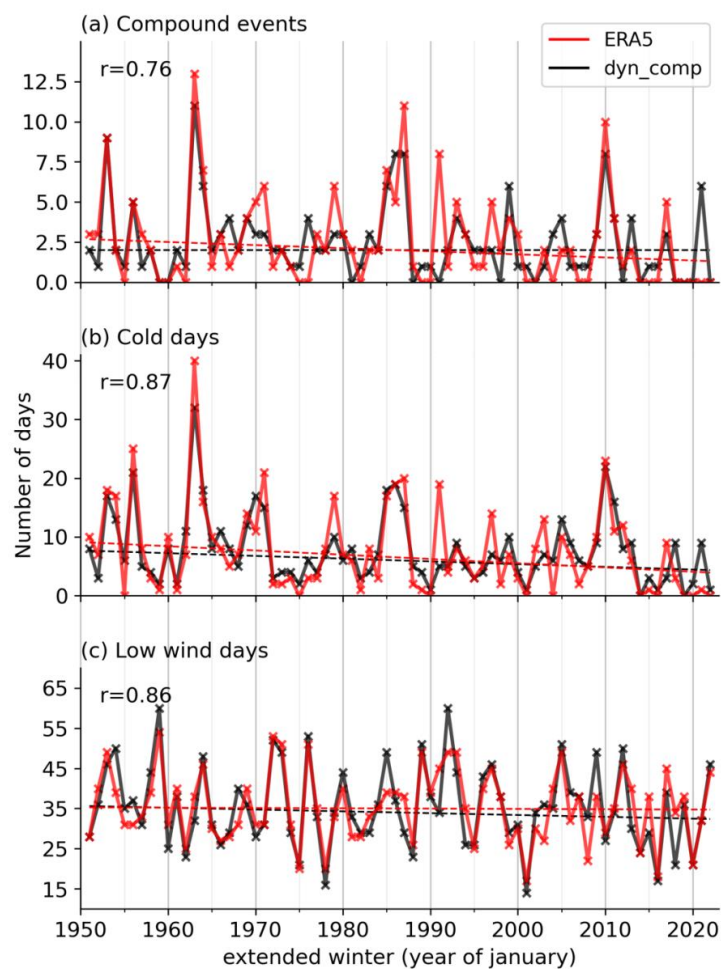
391 Table 2: Trend (slope in days/decade) and associated p-value in the frequency of each weather type (WT; as  
392 defined in Figure 7) in winter over the 1951-2022 period in ERA5. The slope is calculated with the Theil-Sen  
393 estimator and the p-value is calculated with the Mann-Kendall test. Significant trends with  $p < 0.05$  are  
394 highlighted with grey shading.

395

396 Only the frequency of WT4 shows a significant negative trend over the 1951-2022 period (-0.59 day per  
397 decade,  $p=0.01$ ; Table 2). The frequency of WT2 is found to increase (+0.56 day per decade), whereas WT3,  
398 which is associated with the highest frequency of compound events, decreases (-0.27 day per decade) over the  
399 observed period. Trends for both WT2 and WT3 are however not significant.

400 To estimate the contribution of the trends in weather type frequencies on the overall evolution of  
401 compound events, the trends are multiplied by the frequency of compound events for the corresponding  
402 weather type, as done in Horton et al. (2015). Then, the respective contributions from all four weather types  
403 are added to estimate the overall influence of the trends in weather type frequencies. Overall, the trends in  
404 weather type frequencies lead to a weak decrease in the frequency of compound events of 20%. This analysis  
405 suggests a relatively minor influence of large-scale circulation on the trend of compound events. However,  
406 due to significant intra-type variability, a simple change in the frequency of a few weather types may not  
407 capture the full range of circulation changes.

408



409

410 Figure 9: Interannual evolution of the number of (a) compound low wind and cold events, (b) cold days, and  
 411 (c) low wind days in winter over the 1951-2022 period in ERA5 (red) and in their respective dynamic  
 412 components (i.e. dyn\_comp, in black). For each event, the correlation coefficient between ERA5 and their  
 413 respective dynamic components is shown in the upper left. Dashed lines show the linear trend (calculated  
 414 using the Theil-Sen estimator; see Table 3 for the slope value and associated p-value).

	Compound events	Cold days	Low wind days
ERA5	-0.19 (0.02)	-0.72 (0.02)	-0.08 (0.59)
Dynamical component	0.0 (0.10)	-0.47 (0.08)	-0.45 (0.44)

415

416 Table 3: (first row) Trend (slope in days/decade, and associated p-value) in the frequency of low wind days,  
 417 cold days, and compound low wind and cold events in winter over the period 1951-2022 in ERA5 (first row;



418 same trend estimates as in Table 1) and in their respective dynamic component (second row; section 2.7). The  
419 slope is calculated with the Theil-Sen estimator and the p-value is calculated with the Mann-Kendall test.  
420 Significant trends with  $p < 0.05$  are highlighted with grey shading.

421

422 The dynamical adjustment approach described in section 2.7 is now used to better quantify the role of the  
423 large-scale circulation in the evolution of compound low wind and cold events. The interannual variability in  
424 the occurrence of both cold days and low wind days is very well explained by the large-scale circulation  
425 (correlations with the corresponding dynamic component of 0.87 and 0.86, respectively; Figure 9a,b).  
426 Therefore, the interannual variability in the number of compound events is also well explained by the large-  
427 scale circulation (correlations with the corresponding dynamic component of  $r = 0.76$ , Figure 9a). Extreme  
428 winters in terms of compound events such as 1963, 1987, or 2010 are due to a large extent to the atmospheric  
429 circulation. The dynamic component of compound events shows no significant trend over the 1951-2022  
430 period. This suggests that the large-scale circulation has not played an important role in the observed decrease  
431 in the occurrence of compound events. Interestingly, the dynamic component of cold days substantially  
432 decreases (-0.47 days per winter; Table 3), although the p-value does not reach the 0.05 significance level (p-  
433 value=0.08). Large-scale circulation may therefore have contributed to more than 50% of the decline in cold  
434 days occurrence (-0.87 days per winter, Table 3) observed between 1951 and 2022, suggesting that  
435 anthropogenic forcing may not be the only driver of this trend. Finally, there is no significant trend in the  
436 dynamic component of low wind days.

437

#### 438 4. Discussion and conclusions

439 In the context of the energy transition, compound low wind and cold events could present a stronger  
440 threat for the adequacy between the demand and supply in electricity in France. Therefore, it is crucial to  
441 characterize these climate compound events and to better understand how their frequency has changed in the  
442 past to better anticipate how they could evolve in the coming decades.

443

444 Compound low wind and cold events are defined with ERA5 data over the 1950-2022 period using a  
445 wind capacity factor index, and a temperature index that captures the current sensitivity of the electricity  
446 demand in France to temperature. As compound low wind and cold events mainly occur between November  
447 and March, our analyses focus on this period.

448

449 Compound events are quite rare (2 days per winter on average), with a peak occurrence in January.  
450 They are generally short-lived, with a mean duration of 2 consecutive days although they can last up to 13



451 consecutive days. There are large interannual differences in the number of compound events, from 0 to 13  
452 days per winter.

453 Over the observational record, we find a statistically significant decrease in compound events  
454 frequency (-0.19 day per decade) that tends to have amplified over the last four decades. This decrease is likely  
455 driven by the significant negative trend in cold days, while the frequency in low wind days shows no  
456 significant trend. Overall, these results suggest a decrease in climate-related risks for the adequacy between  
457 electricity demand and supply related to compound low wind and cold events over the observed period,  
458 considering the current electricity system.

459 The role of the atmospheric circulation in the occurrence of compound events is assessed using a set  
460 of four weather types derived with the unsupervised k-means classification technique applied to low wind  
461 days. The frequency of compound events in each weather type ranges from 4% to 12%. This reveals a diversity  
462 of regional atmospheric circulations that can lead to the occurrence of compound events in France. The  
463 weather type associated with the highest compound events frequency (WT3) presents pronounced positive  
464 sea-level pressure anomalies over Iceland and negative anomalies west of Portugal. This weather type leads  
465 to negative anomalies of wind speed and temperature throughout Europe, which might pose challenges to the  
466 electricity system on a larger scale than just in France.

467 Overall, we find that the regional atmospheric circulation contributes significantly to the occurrence  
468 of compound events and explains an important part of their interannual variability. Interestingly, the regional  
469 atmospheric circulation shows no significant contribution in the observed decrease in compound events over  
470 the 1951-2022 period in ERA5. In the case of cold days, however, the large-scale circulation might contribute  
471 to approximately 50% of their observed decrease. Similarly, Deser and Phillips (2023) found that large-scale  
472 circulation contributes to a third of the mean winter temperature trend in Europe over the last decades. As  
473 large-scale circulation variability is likely to be largely internal in origin, this result may have implications for  
474 near-term projections.

475

476 In this study, compound low wind and cold events are identified using a straightforward approach that  
477 consists of identifying cold days and low wind days independently. This has the advantage of allowing the  
478 assessment of the relative contribution of cold days and low wind days to the decrease in compound events.  
479 Another approach consists in identifying compound events as days with high residual load (i.e., electricity  
480 demand minus wind power production), i.e., days that need important availability of other power sources than  
481 wind power, such as hydro-electricity or nuclear generation (Bloomfield et al., 2020a). Such approach could  
482 help to test the sensitivity of compound events to different power system scenarios (e.g., with different wind  
483 power installed capacity).

484 With the anticipated rapid increase in onshore and offshore wind farms, the impact of low wind  
485 conditions on French electricity production is expected to increase. Conversely, the impact of cold events on  
486 French electricity demand is expected to decrease due to climate change. The question of how the risk on the



487 adequacy between electricity production and demand associated with compound events will evolve in the next  
488 few decades is therefore multifaceted, depending on both the future level of installed wind power capacity and  
489 climate change. We plan to address this question in future work using climate projections from the latest  
490 Couple Model Intercomparison Project Phase 6.

491 Future risks for the electricity system will also depend on the amount of electricity that can be stored  
492 to modulate the variability of renewable energy production. In this context, long-lasting compound low wind  
493 and cold events at the European scale will be of particular relevance. The study of such long events impacting  
494 a large domain requires a large sample. The use of the ERA5 reanalysis in this context is therefore not  
495 appropriate. An interesting option is to use state of the art Earth System Models, which provide large  
496 ensembles of simulations that enable identifying a higher number of long and high impact compound events  
497 (Bevacqua et al., 2023).

498 How the occurrence of compound events will continue to evolve in a changing climate is also a crucial  
499 question in the context of the energy transition. This study lays a methodological groundwork for addressing  
500 this question. It can also serve as a reference for the evaluation and selection of climate models that could then  
501 be used to assess the projections in compound events. In particular, our findings highlight the important role  
502 of the regional atmospheric circulation in driving compound low wind and cold events in winter in France,  
503 and this contribution is therefore a relevant metric for model evaluation in this context.

504

## 505 **Statements & Declarations**

506 **Fundings.** This study is part of a PhD project funded by Réseau de Transport d'Electricité (RTE).

507 **Competing Interests.** The authors declare they have no conflict of interest.

508 **Author contributions.** All authors contributed to the study conception and design. Data collection and  
509 analysis were performed by FC, MB and JB. All authors contributed to the interpretation of the results. The  
510 first draft of the manuscript was written by FC, MB and JB and all authors commented on previous versions  
511 of the manuscript. All authors read and approved the final manuscript.

512 **Data availability.** The ERA5 reanalysis data is available on the Copernicus Data Store (CDS) at  
513 <https://cds.climate.copernicus.eu/cdsapp#!/dataset/reanalysis-era5-single-levels?tab=overview> (Hersbach et  
514 al., 2020). The MERRA-2 reanalysis data is available from NASA at  
515 [https://disc.gsfc.nasa.gov/datasets/M2T1NXLND\\_5.12.4/summary](https://disc.gsfc.nasa.gov/datasets/M2T1NXLND_5.12.4/summary) (Gelaro et al., 2017). The E-OBS gridded  
516 in situ observation datasets is provided by the European Climate Assessment & Dataset and available at:  
517 <https://www.ecad.eu/download/ensembles/download.php>.

518

519





## 520 References

- 521 Bevacqua, E., Suarez-Gutierrez, L., Jézéquel, A., Lehner, F., Vrac, M., Yiou, P., and Zscheischler, J.:  
522 Advancing research on compound weather and climate events via large ensemble model simulations, *Nat*  
523 *Commun*, 14, 2145, <https://doi.org/10.1038/s41467-023-37847-5>, 2023.  
524
- 525 Bloomfield, H. C., Brayshaw, D. J., and Charlton-Perez, A. J.: Characterizing the winter meteorological  
526 drivers of the European electricity system using targeted circulation types, *Meteorol Appl*, 27,  
527 <https://doi.org/10.1002/met.1858>, 2020a.  
528
- 529 Bloomfield, H. C., Brayshaw, D. J., and Charlton-Perez, A. J.: Characterizing the winter meteorological  
530 drivers of the European electricity system using targeted circulation types, *Meteorol Appl*, 27,  
531 <https://doi.org/10.1002/met.1858>, 2020b.  
532
- 533 Bloomfield, H. C., Brayshaw, D. J., Deakin, M., and Greenwood, D.: Hourly historical and near-future weather  
534 and climate variables for energy system modelling, *Earth Syst. Sci. Data*, 14, 2749–2766,  
535 <https://doi.org/10.5194/essd-14-2749-2022>, 2022.  
536
- 537 Boé, J., Mass, A., and Deman, J.: A simple hybrid statistical–dynamical downscaling method for emulating  
538 regional climate models over Western Europe. Evaluation, application, and role of added value?, *Clim Dyn*,  
539 61, 271–294, <https://doi.org/10.1007/s00382-022-06552-2>, 2023.  
540
- 541 Cassou, C.: Intraseasonal interaction between the Madden–Julian Oscillation and the North Atlantic  
542 Oscillation, *Nature*, 455, 523–527, <https://doi.org/10.1038/nature07286>, 2008.  
543
- 544 Cattiaux, J., Vautard, R., Cassou, C., Yiou, P., Masson-Delmotte, V., and Codron, F.: Winter 2010 in Europe:  
545 A cold extreme in a warming climate, *Geophysical Research Letters*, 37, 2010GL044613,  
546 <https://doi.org/10.1029/2010GL044613>, 2010.  
547
- 548 Cornes, R. C., Van Der Schrier, G., Van Den Besselaar, E. J. M., and Jones, P. D.: An Ensemble Version of  
549 the E-OBS Temperature and Precipitation Data Sets, *JGR Atmospheres*, 123, 9391–9409,  
550 <https://doi.org/10.1029/2017JD028200>, 2018.  
551
- 552 Deser, C. and Phillips, A. S.: A range of outcomes: the combined effects of internal variability and  
553 anthropogenic forcing on regional climate trends over Europe, *Nonlin. Processes Geophys.*, 30, 63–84,  
554 <https://doi.org/10.5194/npg-30-63-2023>, 2023.  
555
- 556 Deser, C., Terray, L., and Phillips, A. S.: Forced and Internal Components of Winter Air Temperature Trends  
557 over North America during the past 50 Years: Mechanisms and Implications\*, *Journal of Climate*, 29, 2237–  
558 2258, <https://doi.org/10.1175/JCLI-D-15-0304.1>, 2016.  
559
- 560 Falkena, S. K. J., de Wiljes, J., Weisheimer, A., and Shepherd, T. G.: Revisiting the Identification of  
561 Wintertime Atmospheric Circulation Regimes in the Euro-Atlantic Sector, *Quart J Royal Meteorol Soc*, 146,  
562 2801–2814, <https://doi.org/10.1002/qj.3818>, 2020.  
563
- 564 Gelaro, R., McCarty, W., Suárez, M. J., Todling, R., Molod, A., Takacs, L., Randles, C. A., Darmenov, A.,  
565 Bosilovich, M. G., Reichle, R., Wargan, K., Coy, L., Cullather, R., Draper, C., Akella, S., Buchard, V., Conaty,  
566 A., Da Silva, A. M., Gu, W., Kim, G.-K., Koster, R., Lucchesi, R., Merkova, D., Nielsen, J. E., Partyka, G.,  
567 Pawson, S., Putman, W., Rienecker, M., Schubert, S. D., Sienkiewicz, M., and Zhao, B.: The Modern-Era  
568 Retrospective Analysis for Research and Applications, Version 2 (MERRA-2), *J. Climate*, 30, 5419–5454,  
569 <https://doi.org/10.1175/JCLI-D-16-0758.1>, 2017.  
570
- 571 Grams, C. M., Beerli, R., Pfenninger, S., Staffell, I., and Wernli, H.: Balancing Europe’s wind-power output  
572 through spatial deployment informed by weather regimes, *Nature Clim Change*, 7, 557–562,



- 573 <https://doi.org/10.1038/nclimate3338>, 2017.  
574
- 575 Hersbach, H., Bell, B., Berrisford, P., Hirahara, S., Horányi, A., Muñoz-Sabater, J., Nicolas, J., Peubey, C.,  
576 Radu, R., Schepers, D., Simmons, A., Soci, C., Abdalla, S., Abellan, X., Balsamo, G., Bechtold, P., Biavati,  
577 G., Bidlot, J., Bonavita, M., Chiara, G., Dahlgren, P., Dee, D., Diamantakis, M., Dragani, R., Flemming, J.,  
578 Forbes, R., Fuentes, M., Geer, A., Haimberger, L., Healy, S., Hogan, R. J., Hólm, E., Janisková, M., Keeley,  
579 S., Laloyaux, P., Lopez, P., Lupu, C., Radnoti, G., Rosnay, P., Rozum, I., Vamborg, F., Villaume, S., and  
580 Thépaut, J.: The ERA5 global reanalysis, *Q.J.R. Meteorol. Soc.*, 146, 1999–2049,  
581 <https://doi.org/10.1002/qj.3803>, 2020.  
582
- 583 Hirschi, J. J. -M. and Sinha, B.: Negative NAO and cold Eurasian winters: how exceptional was the winter of  
584 1962/1963?, *Weather*, 62, 43–48, <https://doi.org/10.1002/wea.34>, 2007.  
585
- 586 Horton, D. E., Johnson, N. C., Singh, D., Swain, D. L., Rajaratnam, B., and Diffenbaugh, N. S.: Contribution  
587 of changes in atmospheric circulation patterns to extreme temperature trends, *Nature*, 522, 465–469,  
588 <https://doi.org/10.1038/nature14550>, 2015.  
589
- 590 Jourdir, B.: Evaluation of ERA5, MERRA-2, COSMO-REA6, NEWA and AROME to simulate wind power  
591 production over France, *Adv. Sci. Res.*, 17, 63–77, <https://doi.org/10.5194/asr-17-63-2020>, 2020.  
592 Lorenz, E. N.: Atmospheric Predictability as Revealed by Naturally Occurring Analogues, *Journal of*  
593 *Atmospheric Sciences*, 26, 636–646, [https://doi.org/10.1175/1520-0469\(1969\)26<636:APARBN>2.0.CO;2](https://doi.org/10.1175/1520-0469(1969)26<636:APARBN>2.0.CO;2),  
594 1969.  
595
- 596 Manwell, J. F.: *Wind Energy Explained: Theory, Design and Application*, n.d.  
597
- 598 Najac, J., Boé, J., and Terray, L.: A multi-model ensemble approach for assessment of climate change impact  
599 on surface winds in France, *Clim Dyn*, 32, 615–634, <https://doi.org/10.1007/s00382-008-0440-4>, 2009.  
600
- 601 Olauson, J.: ERA5: The new champion of wind power modelling?, *Renewable Energy*, 126, 322–331,  
602 <https://doi.org/10.1016/j.renene.2018.03.056>, 2018.  
603
- 604 Otero, N., Martius, O., Allen, S., Bloomfield, H., and Schaeffli, B.: A copula-based assessment of renewable  
605 energy droughts across Europe, *Renewable Energy*, 201, 667–677,  
606 <https://doi.org/10.1016/j.renene.2022.10.091>, 2022a.  
607
- 608 Otero, N., Martius, O., Allen, S., Bloomfield, H., and Schaeffli, B.: Characterizing renewable energy  
609 compound events across Europe using a logistic regression-based approach, *Meteorological Applications*, 29,  
610 <https://doi.org/10.1002/met.2089>, 2022b.  
611
- 612 Plaut, G. and Simonnet, E.: Large-scale circulation classification, weather regimes, and local climate over  
613 France, the Alps and Western Europe, *Clim. Res.*, 17, 303–324, <https://doi.org/10.3354/cr017303>, 2001.  
614 Rapella, L., Faranda, D., Gaetani, M., Drobinski, P., and Ginesta, M.: Climate change on extreme winds  
615 already affects off-shore wind power availability in Europe, *Environ. Res. Lett.*, 18, 034040,  
616 <https://doi.org/10.1088/1748-9326/acbdb2>, 2023.  
617
- 618 Ravestein, P., Van Der Schrier, G., Haarsma, R., Scheele, R., and Van Den Broek, M.: Vulnerability of  
619 European intermittent renewable energy supply to climate change and climate variability, *Renewable and*  
620 *Sustainable Energy Reviews*, 97, 497–508, <https://doi.org/10.1016/j.rser.2018.08.057>, 2018.  
621 Raynaud, D., Hingray, B., François, B., and Creutin, J. D.: Energy droughts from variable renewable energy  
622 sources in European climates, *Renewable Energy*, 125, 578–589,  
623 <https://doi.org/10.1016/j.renene.2018.02.130>, 2018.  
624
- 625 Réseau de Transport d'électricité (RTE): Bilan prévisionnel 2023-2035, 2023.  
626



- 627 Réseau de Transport d'électricité (RTE): Futurs Energétiques 2050 - chapitre 8 (le climat), 2022.  
628
- 629 Saffioti, C., Fischer, E. M., Scherrer, S. C., and Knutti, R.: Reconciling observed and modeled temperature  
630 and precipitation trends over Europe by adjusting for circulation variability, *Geophysical Research Letters*,  
631 43, 8189–8198, <https://doi.org/10.1002/2016GL069802>, 2016.  
632
- 633 Seneviratne, S.I., X. Zhang, M. Adnan, W. Badi, C. Dereczynski, A. Di Luca, S. Ghosh, I. Iskandar, J. Kossin,  
634 S. Lewis, F. Otto, I. Pinto, M. Satoh, S.M. Vicente-Serrano, M. Wehner, and B. Zhou: *Weather and Climate*  
635 *Extreme Events in a Changing Climate.*, 1st ed., Cambridge University Press,  
636 <https://doi.org/10.1017/9781009157896>, 2021.  
637
- 638 Sippel, S., Meinshausen, N., Merrifield, A., Lehner, F., Pendergrass, A. G., Fischer, E., and Knutti, R.:  
639 Uncovering the Forced Climate Response from a Single Ensemble Member Using Statistical Learning, *Journal*  
640 *of Climate*, 32, 5677–5699, <https://doi.org/10.1175/JCLI-D-18-0882.1>, 2019.  
641
- 642 Sippel, S., Fischer, E. M., Scherrer, S. C., Meinshausen, N., and Knutti, R.: Late 1980s abrupt cold season  
643 temperature change in Europe consistent with circulation variability and long-term warming, *Environ. Res.*  
644 *Let.*, 15, 094056, <https://doi.org/10.1088/1748-9326/ab86f2>, 2020.  
645
- 646 Staffell, I. and Pfenninger, S.: Using bias-corrected reanalysis to simulate current and future wind power  
647 output, *Energy*, 114, 1224–1239, <https://doi.org/10.1016/j.energy.2016.08.068>, 2016.  
648
- 649 Tedesco, P., Lenkoski, A., Bloomfield, H. C., and Sillmann, J.: Gaussian copula modeling of extreme cold  
650 and weak-wind events over Europe conditioned on winter weather regimes, *Environ. Res. Let.*, 18, 034008,  
651 <https://doi.org/10.1088/1748-9326/acb6aa>, 2023.  
652
- 653 Terray, L.: A dynamical adjustment perspective on extreme event attribution, *Weather Clim. Dynam.*, 2, 971–  
654 989, <https://doi.org/10.5194/wcd-2-971-2021>, 2021.  
655
- 656 Thornton, H. E., Scaife, A. A., Hoskins, B. J., and Brayshaw, D. J.: The relationship between wind power,  
657 electricity demand and winter weather patterns in Great Britain, *Environ. Res. Let.*, 12, 064017,  
658 <https://doi.org/10.1088/1748-9326/aa69c6>, 2017.  
659
- 660 Van Den Dool, H. M.: Searching for analogues, how long must we wait?, *Tellus A*, 46, 314–324,  
661 <https://doi.org/10.1034/j.1600-0870.1994.t01-2-00006.x>, 1994.  
662
- 663 Van Oldenborgh, G. J., Mitchell-Larson, E., Vecchi, G. A., De Vries, H., Vautard, R., and Otto, F.: Cold  
664 waves are getting milder in the northern midlatitudes, *Environ. Res. Let.*, 14, 114004,  
665 <https://doi.org/10.1088/1748-9326/ab4867>, 2019.  
666
- 667 van der Wiel, K., Stoop, L. P., van Zuijlen, B. R. H., Blackport, R., van den Broek, M. A., and Selten, F. M.:  
668 Meteorological conditions leading to extreme low variable renewable energy production and extreme high  
669 energy shortfall, *Renewable and Sustainable Energy Reviews*, 111, 261–275,  
670 <https://doi.org/10.1016/j.rser.2019.04.065>, 2019a.  
671
- 672 van der Wiel, K., Bloomfield, H. C., Lee, R. W., Stoop, L. P., Blackport, R., Screen, J. A., and Selten, F. M.:  
673 The influence of weather regimes on European renewable energy production and demand, *Environ. Res. Let.*,  
674 14, 094010, <https://doi.org/10.1088/1748-9326/ab38d3>, 2019b.  
675
- 676 Zscheischler, J., Martius, O., Westra, S., Bevacqua, E., Raymond, C., Horton, R. M., van den Hurk, B.,  
677 AghaKouchak, A., Jézéquel, A., Mahecha, M. D., Maraun, D., Ramos, A. M., Ridder, N. N., Thiery, W., and  
678 Vignotto, E.: A typology of compound weather and climate events, *Nat Rev Earth Environ*, 1, 333–347,  
679 <https://doi.org/10.1038/s43017-020-0060-z>, 2020.  
680